This is a previous version of the article published in Russian Journal of Electrochemistry. 2016, 52(9): 890-900. doi:10.1134/S1023193515110117

Cu UPD at Pt(100) and stepped faces Pt(610), Pt(410) of platinum single crystal electrodes.

E.B. Molodkina, A.I. Danilov, J.M. Feliu*

A. N. Frumkin Institute of Physical Chemistry and Electrochemistry, Russian Academy of Sciences, Moscow, Russia

* Institute of Electrochemistry, University of Alicante, Alicante, Spain

ABSTRACT

The processes of adsorption/desorption of copper adatoms on the basal Pt(100) face and stepped Pt(610), Pt(410) surfaces have been studied in perchloric acid solution by cyclic voltammetry. It has been shown that the positions of the Cu stripping peaks are determined by perfection of the adlayer. The "island" model is suggested to describe electrochemical behavior of the Pt(hkl)+Cu_{ad} system. Obtained results are important for target modification of shape-controlled nanoparticles that are used in electrocatalysis.

Key words: Pt(100), Pt(610), Pt(410), Cu adatoms, perchloric acid solutions.

Corresponding author: **A.I. Danilov,** e-mail: danilov@phyche.ac.ru, alex_ipc@mail.ru

INTRODUCTION

It is known that modification of noble metal surfaces by adatoms is an effective method of increasing the catalytic activity of electrode substrates [1, 2]. Kinetics and mechanism of nitrate reduction in electrochemical systems were studied in detail on different polycrystalline electrodes modified by adatoms of copper, lead, tin, germanium etc. [3–16]. Bimetallic catalysts, e.g., Pt–Ge, Pt–Cu, Pd–Ge, Pd–Cu etc. are often used to enhance the reduction rate of nitrate ions [4–7, 12–16]. It was found that nitrate ions are not reduced by dissolved hydrogen on pure platinum (θ_{Cu}=0), but maximal high catalytic activity is observed at medium surface coverage of copper adatoms (0.5–0.6 monolayer) [16].

On the other hand, using single crystal electrodes (bulk crystals and shape-controlled nanoparticles) is of greatest interest as most of electrocatalytic reactions are structure-sensitive. Consequently, there is a possibility to establish a correlation between the structure of adsorption sites and their catalytic activity [17–29]. Our previous studies of nitrate reduction on Pt(111) and Pt(111) + Cu electrodes [22] have shown that sulfate anions block the adsorption sites on the surface of the modified electrode, thus hindering the adsorption of nitrate anions and their reduction. The extent of inhibition slightly depends on the copper adatom coverage. Nitrate reduction on Cu-modified Pt(111) electrodes in perchloric acid solutions occurs much faster as compared with pure platinum, the steady state currents are higher by several orders of magnitude. The catalytic effect of copper adatoms is largely caused by the facilitation of nitrate adsorption (induced nitrate adsorption) as the copper adatoms have a partial positive charge [23] due to a shift of electron density from Cu to Pt atoms (formation of Cu adatom from Cu^{2+} ion really takes of 2-electron transfer). Hydrogen adatoms block the adsorption sites on platinum for nitrate adsorption and inhibit nitrate reduction even at moderate surface coverage.

The results of a detailed study of the nitrate reduction mechanism at the Pt(100) and Pt(100)+Cu electrodes were reported in [24, 25]. It was shown that modification of Pt(100) with Cu adatoms also produces a significant effect on the kinetics of nitrate and nitrite electroreduction as compared with unmodified electrodes.

Methodological aspects of modification of platinum single crystals by Cu adatoms and crystallites were discussed in [29].

The results of Cu UPD studies on stepped surfaces of platinum single crystals Pt[n(100)x(110)] and Pt[n(100)x(111)] ((100) terraces of various width separated by parallel monoatomic height steps with (110) or (111) orientation, respectively) in solutions with strongly adsorbed anions, sulfate or chloride, were given in Refs. [30, 31]. Analysis of the changes in the shape of CVs in the hydrogen region in the course of copper adatoms accumulation from diluted solutions has shown that at the initial stages of Cu deposition (low surface coverage θ_{Cu}) copper adsorption occurs simultaneously on the (100) terraces and (110) steps [30]. It was concluded [31] that on the stepped surfaces with (111) steps deposition of Cu adatoms occurs preferably on the (100) terraces but not on the steps. The peak of copper desorption from the steps is located at less positive potentials than that from the terraces. One can assume that (111) steps are blocked by strongly adsorbed anions in a considerable extent.

Our previous studies of Cu UPD on stepped faces of single crystals Pt(554) and Pt(775) with (111) terraces and (110) steps, using electrochemical measurements [32] and quantum-chemical calculations [33], have shown that the peak of Cu desorption from the steps is located at more positive potentials than that from the terraces. The energy of Cu_{ad} interaction with the surface depends on the amount of Pt atoms contacting the Cu atom. On hexagonal (111) terraces Cu atom contacts with three Pt near neighbor atoms but on the (110) steps – with five Pt atoms. It means that Cu adatoms are more strongly adsorbed at the steps and thus the peak of Cu desorption from the steps is located at more positive potentials.

In this paper, the processes of copper adsorption/desorption on Pt(100), Pt(610) and Pt(410) faces in perchloric acid solution (weakly adsorbed anion) with addition of 0.01 mM copper ions are considered. It is shown that at the initial stages of the process the positions of the Cu desorption peaks are determined by perfection of the adlayer to a great extent.

EXPERIMENTAL

The electrodes, with a working surface area of 0.03–0.04 cm^2 were prepared in University of Alicante (Spain) using the technique developed by Clavilier et al. [34–36]. Prior to the experiments, the electrodes were annealed for 20–40 s in the flame of a Bunsen burner to remove impurities and to order the surface structure. After that, the electrodes were cooled in an argon–hydrogen gas mixture (3:1), rinsed with Milli-Q water saturated by this mixture andtransferred into a cell, filled with 0.1 M $HClO_4$ solution degassed by argon, protected with a drop of water. Then a hanging electrode/solution meniscus (this configuration provides a contact of only a working face of a single crystal with the solution) was formed at 0.05 V, and blank cyclic voltammograms (CVs) were recorded to control the system purity and the quality of the electrode annealing/cooling treatment. All the CVs were recorded at the sweep rate of 50 mV/s.

Measurements were performed in glass cells with separate compartments for an auxiliary Pt electrode and reversible hydrogen electrode (RHE). The solutions were prepared on the basis of CuO (“p.a.” grade, Merck), $HClO_4$ (“suprapure” grade, Merck) and Milli-Q water (Millipore) with specific resistance of 18 MOhm cm and

content of organic impurities of less than 5 ppb. Only this water was used for cell cleaning, electrode rinsing, etc. High-purity argon was used to deaerate the solution; the inert gas was blown over the solution in the course of the experiments. To introduce an copper perchlorate additive, the meniscus was broken and the electrode was left above the solution in the argon atmosphere. After adding an aliquot of the solution, argon was bubbled through the electrolyte for 2-3 minutes to level the additive bulk concentration and remove oxygen traces from the system. Then, a meniscus was formed again at 0.8 V, potential cycling was resumed, and CVs were recorded.

A computer-controlled potentiostat and software developed at IPCE RAS were used for data recording and processing.

RESULTS AND DISCUSSION

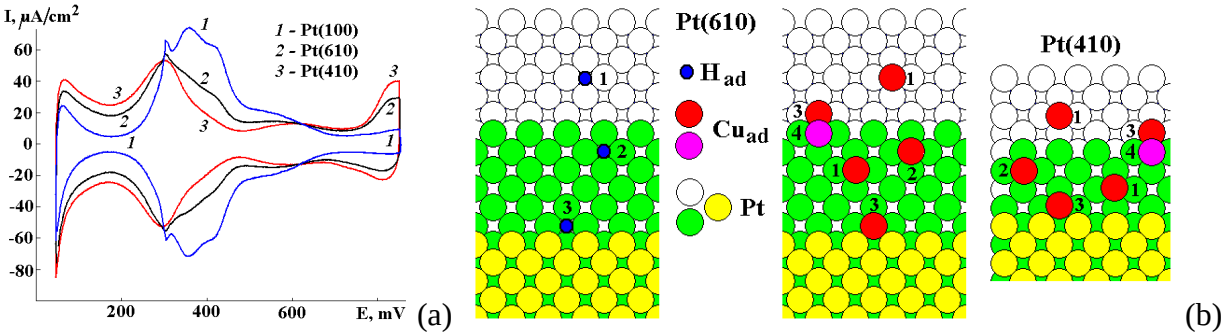

Fig. 1. (a) Blank CVs of Pt(100), Pt(610) and Pt(410) in 0.1 M $HClO_4$. (b) Surface structure of the stepped faces. Location of H_{ad} or Cu_{ad}: *1* - on the terraces, *2* - on the terrace borders, *3* - at the steps (primary step decoration), *4* - secondary decoration of the steps.

Blank CVs of studied electrodes in the perchloric acid test solution are presented in Fig. 1a. The surface structure of the ideal stepped surfaces is schematically shown in Fig. 1b. The terrace width of real electrodes is n±1 atom. In previous contributions [31, 37], it was found that hydrogen adsorption/desorption occurs at the steps at potentials below 0.2 V, on the terrace borders at 0.2-0.3 V, and in the middle of (100) terraces at 0.3-0.5 V (Fig. 1b). One can see a small peak in the CV of Pt(100) at 0.3 V, it is always observed even for high-quality single crystals. It was shown in Ref. [38] that after annealing/cooling of Pt(100) there are few square islands and holes of monoatomic height on the wide terraces of the surface. Consequently, there is a certain amount of adsorption sites at the steps, which are coming from defects of the surface structure.

Comparison of CVs in Fig. 1a shows that the currents at E<0.3 V grow with a decrease of the terrace width (increase of the step density) and fall in the region 0.3-0.5 V. The potential region of 0.5-0.7 V corresponds to adsorption/desorption of intermediate products of water oxidation (OH_{ad}-species on the terraces), and at more positive potentials adsorbed oxygen is present on the surface of the electrodes. With an increase in the step concentration, the amount of O_{ad} rises and the currents at E>0.7 V grow. One can conclude that O_{ad} is present mainly at the steps or on the terrace borders.

Use of diluted solutions (concentration is lower than 0.1 mM Cu^{2+}) allows smoothly increasing the surface coverage of copper adatoms as the UPD process is controlled by mass transfer (diffusion) in the whole potential range. The results of the potentiodynamic experiments on slow accumulation of Cu_{ad} on Pt(610) (6-atomic terraces) are presented in Fig. 2. The meniscus was formed at 0.85 V, then 3 cycles of 850-600 mV were applied at 50 mV/s, and further the potential was cycled between 600 and 50 mV (30 cycles correspond to a total time interval of copper deposition of 660 s). After a fixed number of the Cu_{ad} accumulation cycles, again 3 cycles of 850-600 mV were applied to control the amount of adsorbate and to remove the excess of copper ions from the near-electrode layer of the solution. Integration of the final first positive going sweep from 50 to 600 mV and the following sweep from 600 to 850 mV with subtracting of the blank CV (Fig. 2c, account of double layer capacity charging and currents of oxygen adsorption) allows estimating the number of adsorption sites blocked by Cu_{ad} (ΔQ_1, ΔQ_2, ΔQ_3) and the surface coverage θ_{Cu} ($Q=\Delta Q_4+\Delta Q_5$, Figs. 2c, 2d). The measured charges amount to 408-420 $\mu C/cm^2$ and correspond to the desorption of a complete copper monolayer (θ_{Cu}=1 ML) from the surfaces of Pt(410), Pt(610) and Pt(100) (one Cu adatom on each surface Pt atom taking into account secondary decoration of the steps [32], Figs. 1b, 2e, positions *4*).

The changes in the shape of the CVs in the hydrogen region (E<0.5 V, Figs. 2a, 2c) allow concluding that deposited copper atoms block adsorption sites for hydrogen adatoms both at the steps and on the terraces. One can see that the double peak of copper desorption from the steps and terraces (Figs. 2b, 2c) is observed only for θ_{Cu}<0.4 ML (5-8 cycles of copper accumulation, deposition time up to 3 min). Analysis of the charge balance shows that $2\Delta Q_1 \approx \Delta Q_4$ and $2(\Delta Q_2 + \Delta Q_3) \approx \Delta Q_5$ (Fig. 2c). Although the estimation is very rough, it means nevertheless that the sharp peak at 0.68 V (Figs. 2b, 2c) corresponds to the copper desorption from the steps and the peak at 0.72 V is due to the copper desorption from the terraces. This correlates with the results reported in previous studies [30, 31].

In the case of the Pt(554) and Pt(775) electrodes, double peaks of copper desorption from (110) steps and (111) terraces were observed even for θ_{Cu}=1 ML, but copper desorption from the steps took place at more positive potential than that from the terraces [32].

It is worth to note the positive shift of Cu desorption peaks with the increase of θ_{Cu} (Fig. 2b). It is expected that removing isolated adatoms (Fig. 2e, positions *1*, *2*) is simpler than destroying the islands on the terraces (with the anions on the surface of the islands that stabilize the adatoms inside the islands, Fig. 2e, positions *2a*) or a continuous row of the adatoms on the steps (Fig. 2e, positions *1a*, on the terrace borders the anions could be adsorbed as well). Most probably, this positive shift of the desorption peaks with the increase in θ_{Cu} is due to the growth of the island size and the decrease in number of the islands of Cu_{ad} , as a result of their coalescence. If the island on the terrace contacts a row of adatoms on the step (Fig. 2e, stage C, high surface coverage), only a single peak of copper desorptive stripping is observed at potentials of 0.75-0.8 V: it corresponds to the removal of the whole complex set of adatoms from the terrace and step. Most probably, desorption of such complexes begins at the perimeter of the islands on the terrace (Fig. 2e, stage C, positions *3*, *4*). The anodic peak of Cu desorption at E<0.72 V could be attributed to the removal of isolated adatoms from the steps (Fig.

2e, stages A, B, positions *1*). The positive shift of these peaks with the increase of θ_{Cu}, is probably due to formation of the sections of continuous rows of Cu_{ad} at the steps and islands on the terraces (Fig. 2e, stage B).

It is worth to note that after long-term Cu accumulation (15-30 cycles, Fig. 2b) the desorption peak shifts in the positive direction and decreases in height with the increase of θ_{Cu}. In addition, an increase in currents at 640-740 mV is observed (Fig. 2b) due to elimination of the secondary step decoration (Fig. 2e, stage C, position *4*).

Our quantum-chemical calculations and modeling of the process of Cu adlayer formation have shown [33] that interaction Pt-Cu is energetically favorable, but as the adatoms have a partial positive charge [23], at the initial stages of the adsorption only isolated copper adatoms are located on the surface of the terraces and steps (Fig. 2e, stage A, positions *1,2*). In this case their mutual electrostatic repulsion gives a minimal contribution to the increase in the surface energy of the system. For high θ_{Cu} and presence of many Cu_{ad} islands it is necessary to take into account the stabilizing role of anions adsorbed on these islands. Although perchlorate anions are weakly adsorbed on platinum, their eventual adsorption on the partly positive charged copper adlayer could be induced.

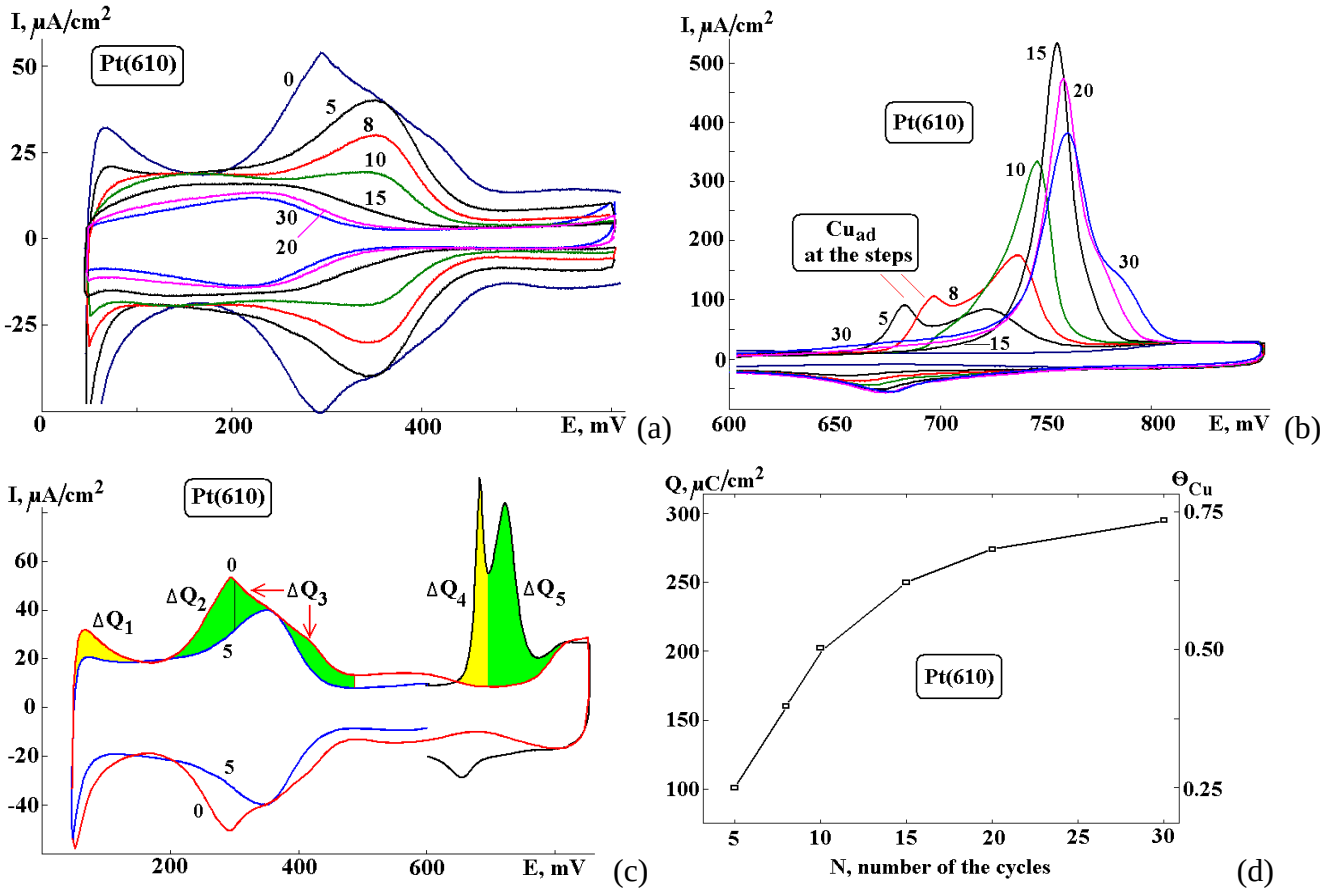

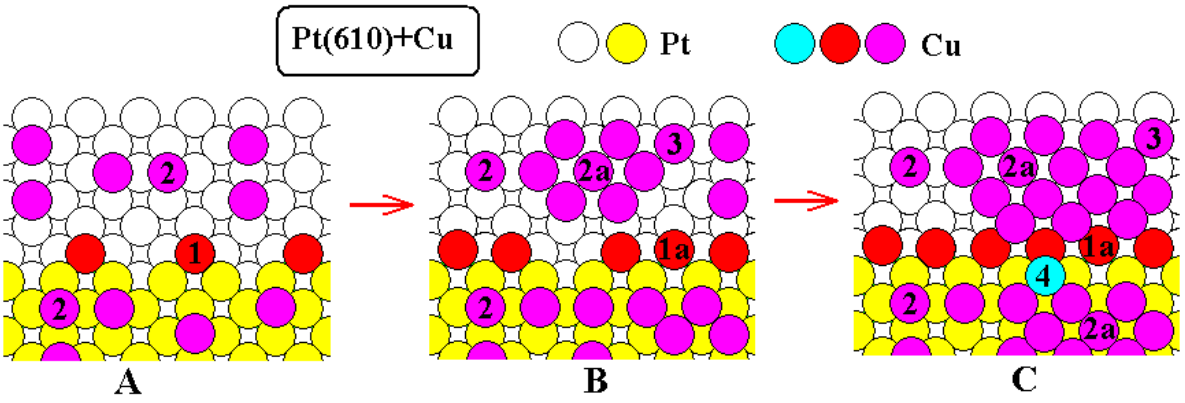

(e)

Fig. 2. CVs of Pt(610) after 5-30 cycles of Cu_{ad} accumulation in solution of 0.1 M $HClO_4$ + 0.01 mM $Cu(ClO_4)_2$ in the range of 50-600 mV. (a) Final cycles of 50-600 mV. 0 – blank CV of Pt(610) in the solution of 0.1 M $HClO_4$. (b) First cycles of 600-850 mV. Number of accumulation cycles is pointed out in the plots. (c) Blank CV (0), 5th cycle of 50-600 mV and 1st cycle of 600-850 mV (5). (d) Charges Q of Cu desorption at 600-850 mV (with subtracting the blank CV). (e) The sketch of the adlayer formation. The explanations are in the text.

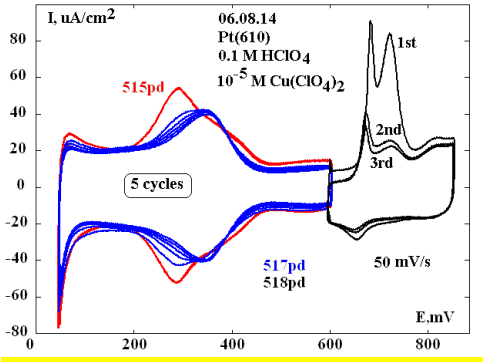

comment

In another series of the experiments the accumulation of Cu_{ad} on all studied electrodes was carried out in the potential range of 50-350 mV at 50 mV/s, using the polarization program shown in Fig. 3, which ensured obtaining the reproducible data. After desorption of accumulated copper at 650-850 mV, the concentration of Cu^{2+} in the near-electrode layer is higher than in the bulk of the solution and this effect can be observed in the CVs of the second and third cycles of 600-850 mV (not shown, an enhanced amount of Cu is adsorbed/desorbed in this potential range as compared with the case of the potential cycling without previous accumulation of Cu_{ad}). To level the copper concentration in the upper layer of the solution, the meniscus was broken at 850 mV, argon was bubbled into the solution for 1 min, the meniscus was formed again at 800 mV several times (removing the drop of solution with enhanced concentration of Cu^{2+} from the electrode surface) and then the standard pretreatment was performed (10 cycles 800-600 mV). At this stage, formation of some amount of copper oxides is possible (coadsorption of Cu_{ad} and O_{ad}), which are the active centers for copper deposition [32, 39]. The next accumulation of copper adatoms was started only after this pretreatment (Fig. 3). During the potential cycling between 50 and 350 mV partial or complete reduction of copper oxides could occur as a result of oxygen desorption.

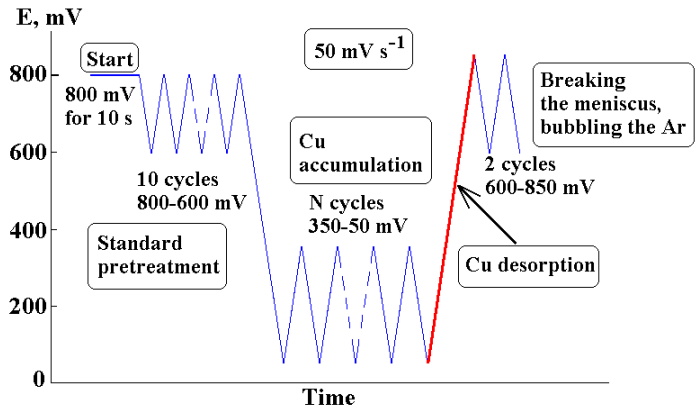

Fig. 3. The sketch of polarization program of the electrodes.

Detailed data on the initial stages of copper accumulation on Pt(610) are presented in Fig. 4. Similar to the CVs in Fig. 2, double peaks of Cu_{ad} desorption from the terraces and steps are observed. Mentioned above explanations are also suitable in this case. It is worth to note that 10 cycles in the range of 50-350 mV correspond to 2 min of copper deposition and a desorption charge of ca. 160 μC/cm^2 (θ_{Cu}≈0.4 ML).

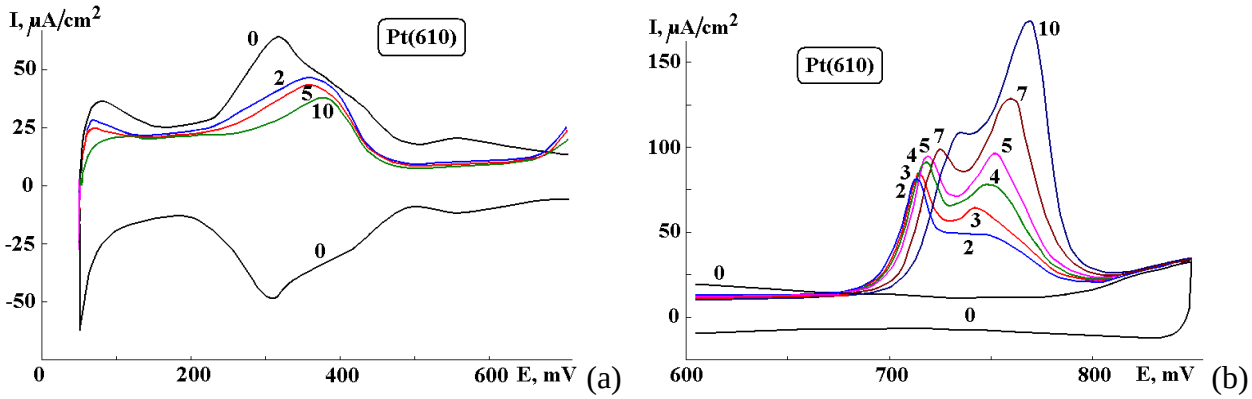

Fig. 4. Fragments of positive-going CV sweeps of Pt(610) after 2-10 cycles of copper accumulation in solution of 0.1 M $HClO_4$ + 0.01 mM $Cu(ClO_4)_2$ in the range of 50-350 mV. (a) Changes in hydrogen region (b) The curves of copper desorption. The number of copper accumulation cycles is pointed out at the plots. 0 – blank CV of Pt(610) in solution of 0.1 M $HClO_4$.

At the voltammograms of Cu desorption from Pt(410) (4-atomic terraces, Fig. 5) the double peak is observed after accumulation up to 0.2 ML of adatoms (after 5 cycles 50-350 mV only a shoulder at 0.72 V is observed in the curve of copper desorption). Apparently, the islands of copper adatoms on narrow terraces are formed at very early stages of the deposition process (Fig. 5c). Similar to the CVs from Pt(610), the peak of copper desorption from Pt(410) shifts in the positive direction with the increase in θ_{Cu} and the corresponding increase in the extent of the adlayer ordering.

It is worth to note the enhanced anodic currents at 650-750 mV after long-term copper accumulation (Figs. 5a, 5b). Previously we observed the processes of secondary decoration of the steps for the electrodes with (111) terraces [32]. Apparently, a similar process takes place at stepped surfaces with (100) terraces (position *3* in sketch 5c).

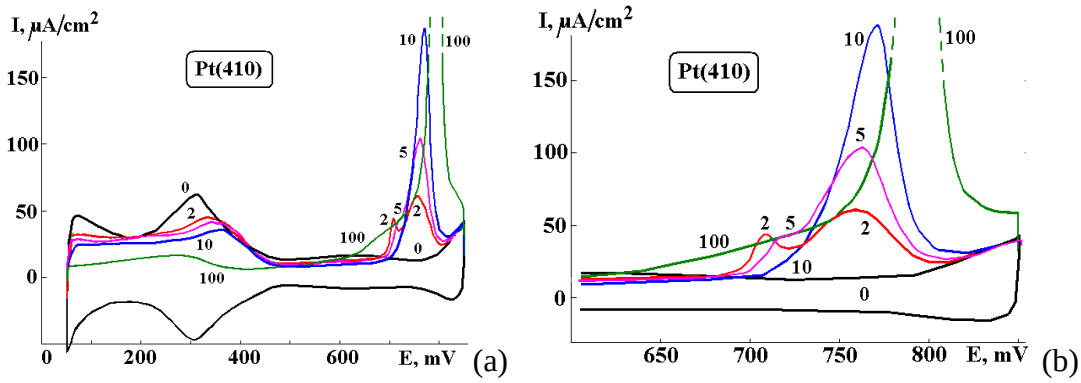

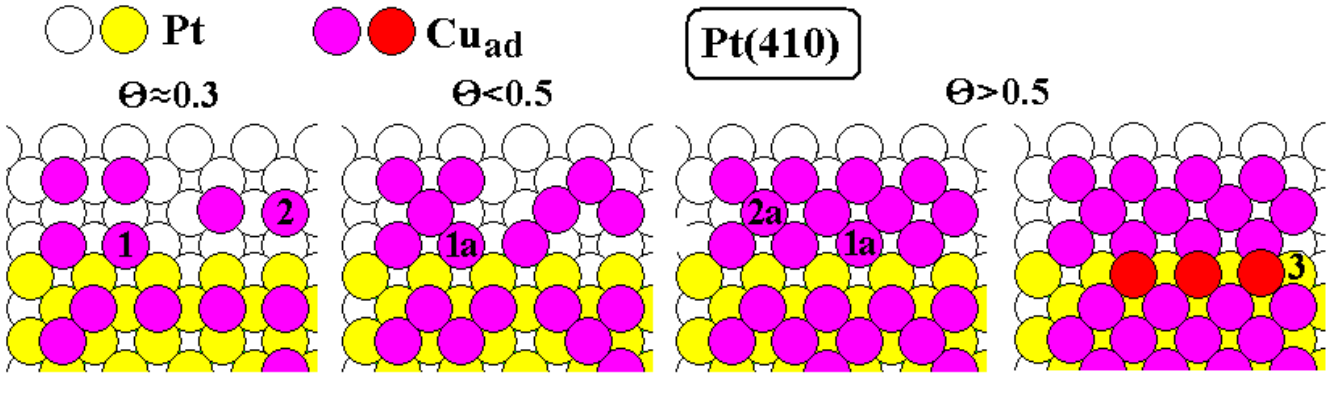

Fig. 5. CVs of Pt(410) after 2-100 cycles of copper accumulation in solution of 0.1 M $HClO_4$ + 0.01 мМ $Cu(ClO_4)_2$ in the range of 50-350 mV. (a) Positive-going sweeps 50-850 mV. (b) Fragments of these sweeps in enlarged scale. The number of copper accumulation cycles is pointed out at the plots. 0 – blank CV of Pt(410) in solution of 0.1 M $HClO_4$. (c) The sketch of the adlayer formation. Location of Cu_{ad}: *1* - at the steps (primary step decoration), *2* - on the terraces, *3* - secondary decoration of the steps.

The presence of double peaks of copper desorptive stripping in the CVs of stepped surfaces of platinum single crystals is quite regular. However, we have observed for the first time distinct double peaks for this process from the most uniform surface of Pt(100) at θ_{Cu}>0.5 ML (30 cycles of 50-350 mV). At the initial stages of copper accumulation, a single desorption peak is observed at 0.73 V (10 cycles, Fig. 6a). After 25 cycles of copper accumulation, this peak is lower and shifts slightly (0.74 V). However, a shoulder at 0.8 V appears (the desorption charge is higher than 200 μC/cm^2, θ_{Cu}≈0.5 ML, Fig. 7d). Further accumulation of Cu_{ad} leads to a decrease in currents of hydrogen adsorption/desorption (Fig. 7a), an increase in the desorption peak at 0.8-0.83 V and a decrease in the shoulder at less positive potentials (Fig.6).

The explanation of this effect is also possible on the basis of the "island" model of the adlayer formation (Fig. 6b). At the initial stages of copper accumulation on the Pt(100) surface, mainly isolated adatoms are present, their desorption taking place at E<0.75 V. With the increase in θ_{Cu} up to 0.5 ML (30 cycles of copper accumulation), the islands of the adlayer begin to form, the remaining isolated adatoms and adatoms at the perimeter of the islands desorb at different potentials. At high θ_{Cu}, islands are mainly present on the surface, the potential of Cu_{ad} desorption shifts in the positive direction with increase in the extent of the adlayer ordering.

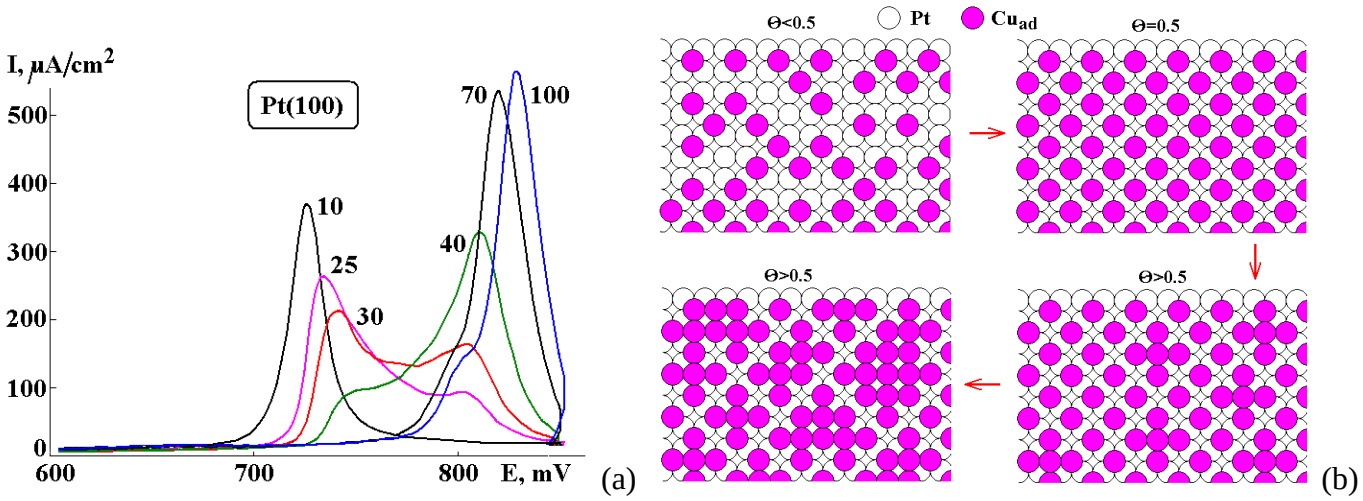

Fig. 6. (a) Fragments of CV positive-going sweeps of Pt(100) after 10-100 cycles of copper accumulation in solution of 0.1 M $HClO_4$ + 0.01 мМ $Cu(ClO_4)_2$ in the range of 50-350 mV. The number of copper accumulation cycles is pointed out at the plot. (b) The sketch of the adlayer formation.

The comparison of the positive-going sweeps of CVs after 10-100 cycles of Cu accumulation in the range of 50-350 mV for all studied electrodes is shown in Fig. 7. One can see (Fig. 7a), that the maximal blocking of the surface for hydrogen adsorption is observed for Pt(100), and the minimal one is found for Pt(410), with contains narrow 4-atomic terraces, for the same duration of Cu deposition. This fact is confirmed by integration of the desorption curves (Fig. 7d). The desorption peak in Fig. 7b for 10 cycles of Cu accumulation on Pt(100) is located at less positive potentials than on other electrodes and corresponds to removing the isolated copper adatoms. For these conditions, the adlayer on Pt(410) evidently contains islands (see also Fig. 5). After 30 cycles of copper accumulation (Fig. 7b) on Pt(100) there are both isolated adatoms and islands of Cu_{ad} ladayer, but on Pt(610) and Pt(410) – only the islands. After more long-term Cu deposition (Fig. 7c), mainly the islands of Cu adlayer are present on the electrode surfaces and their removal occurs at more positive potentials from Pt(100) (curves *1*) than that for stepped surfaces (curves *2,3*). This is due to a higher ordering of the Cu adlayer on Pt(100), as compared with the Pt(610) and Pt(410) stepped surfaces.

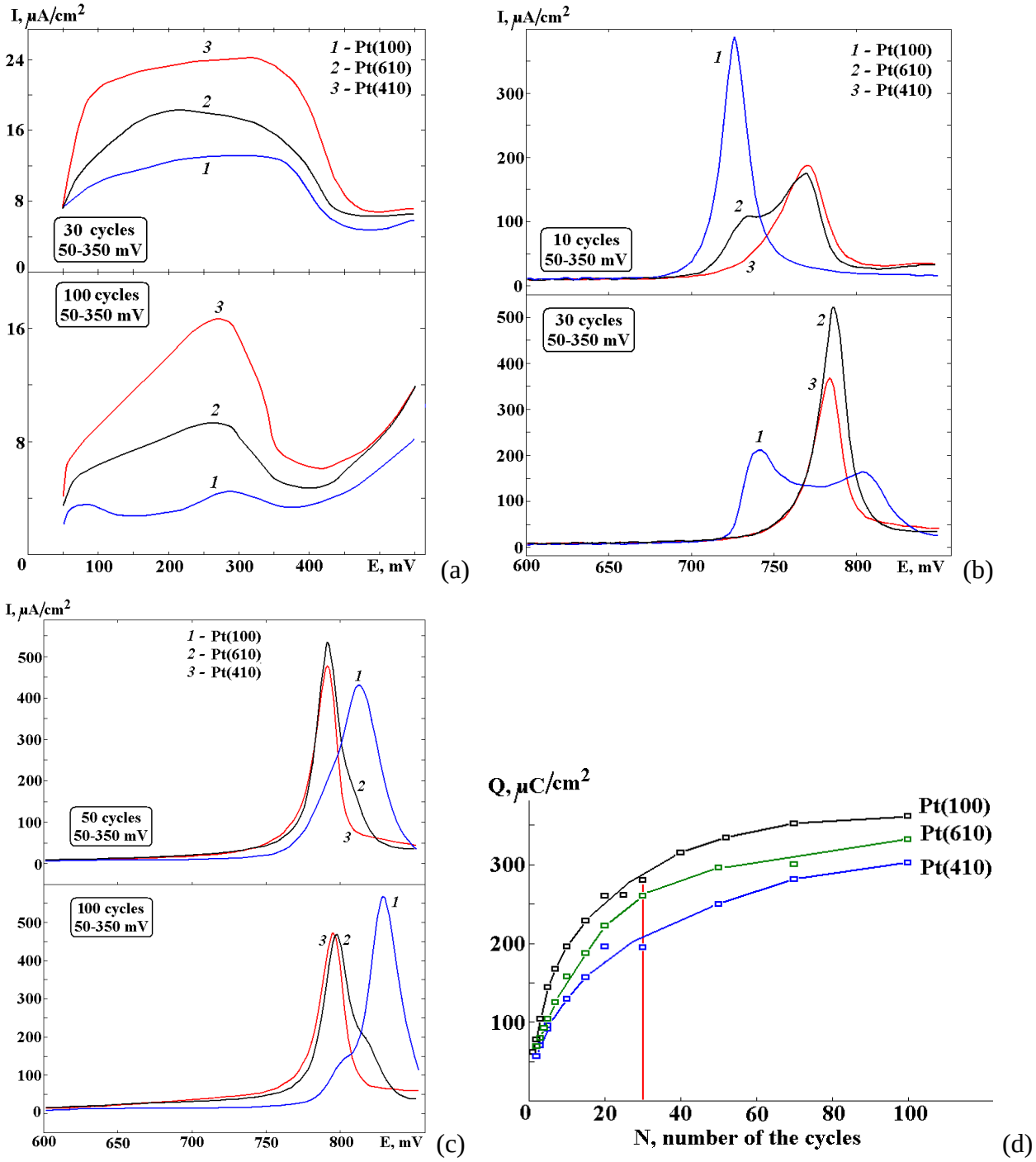

Fig. 7. (a-c) Fragments of CV positive-going sweeps of Pt(100), Pt(610) and Pt(410) after 10-100 cycles of copper accumulation in solution of 0.1 M $HClO_4$ + 0.01 мМ $Cu(ClO_4)_2$ in the range of 50-350 mV. The number of copper accumulation cycles is pointed out at the plots. Polarization program is shown in Fig. 3. (a) Hydrogen region. (b,c) The peaks of Cu desorption. (d) The dependences of amount of desorbed copper from the number of the 50-350 mV cycles of copper accumulation (the charges of Cu desorption were calculated after subtraction of the blank CVs).

Special explanations are necessary for the data in Fig. 7d and it is important to understand why:

(1) the Q(N) curves have a plateau, which corresponds to $\theta_{Cu} < 1$ ML;

(2) the rate of Cu deposition decreases with increase in the step site concentration?

The answer to the first question is almost evident: considerable depletion of near-electrode layer of the solution. According to Cottrell equation the thickness of diffusion layer grows with time and the rate of an electrochemical process decreases. One should also take into account that the steps could be blocked partly by adsorbed oxygen or copper oxides.

However, the second question is more complicated. The depletion of the near-electrode layer of the solution for Pt(410) is lower than that for Pt(100) and Pt(610) as the rate of Cu deposition on Pt(410) is the lowest (Fig. 7d, differential coefficients dQ/dt or dQ/dN are proportional to the Cu deposition rate). Thus in this case this factor is not decisive. It should be taken into account that for the stepped surfaces Pt[n(100)x(110)] the potential of zero total charge decreases with an increase in the of step density [40]. Consequently, the adsorption of copper ions is hindered on Pt(410) and Pt(610) as compared with Pt(100) and the rate of charge transfer for these stepped surfaces is lower for the same potentials. It is also important to consider the fact of positively charged copper adlayer [23] due to a shift of electron density from Cu to Pt atoms. In the limited space of narrow terraces the mutual repulsion of Cu atoms could be a decisive factor for the adsorption sequence (compare the sketches in Figs. 5c and 6b). This could be one of the causes for the decrease in copper accumulation rate with time.

CONCLUSIONS

The performed studies of the initial stages of Cu UPD on the basal Pt(100) face and stepped Pt(610), Pt(410) faces in diluted Cu^{2+} solution allows concluding that the positions of Cu desorption peaks are determined to a great extent by the perfectness of the the adlayer structure. At low surface coverages θ_{Cu} copper desorption from the steps (110) occurs at lower potentials than that from the (100) terraces. Double peaks of copper desorption are observed even for the energetically uniform surface of Pt(100) electrode – the desorption of isolated Cu adatoms occurs at less positive potentials than that of the Cu_{ad} islands. The “island” model of the adlayer formation allows explaining all the observed effects in the studied system Pt(hkl)+Cu_{ad}.

ACKNOWLEDGMENTS

Financial support from the Russian Foundation for Basic Research (project no. 14-03-00530), MINECO (CTQ2013-44083-P) and Generalitat Valenciana (PrometeoII/2014/013) (Feder, Spain) is gratefully acknowledged.

REFERENCES

1. Adzic, R., *Advances in Electrochemistry and Electrochemical Engineering.* Ed. Gerischer H., N.Y.: Wiley and Sons, 1984, vol. 13. p. 159.

2. Petrii, O.A., and Tsirlina, G.A., *Itogi Nauki I Tekhmiki. Elektrokhimiya.* Moscow: VINITI. 1988, vol. 27, p. 3.

3. De Groot, M.T., and Koper, M.T.M., *J. Electroanal. Chem.*, 2004, vol. 562, p. 81.

4. Petrii, O.A., and Safonova, T.Ya., *J. Electroanal. Chem.*, 1992, vol. 331, p. 897.

5. Safonova, T.Ya., and Petrii, O.A., *J. Electroanal. Chem.*, 1998, vol. 448, p. 211.
6. Gootzen, J.F.E., Peeters, P.G.J.M., Dukers, J.M.B., Lefferts, L., Visscher, W., and van Veen, J.A.R., *J. Electroanal. Chem.*, 1997, vol. 434, p. 171.
7. Gootzen, J.F.E., Lefferts, L., and van Veen, J.A.R., *Appl. Catal. A: General*, 1999, vol. 188, p. 127.
8. De Vooys, A.C.A., van Santen, R.A., and van Veen, J.A.R., *J. Mol. Catal*., 2000, vol. 154, p. 203.
9. Da Cunha, M.C.P.M., Weber, V., and Nart, F.C., *J. Electroanal. Chem.*, 1996, vol. 414, p. 163.
10. Da Cunha, M.C.P.M., De Souza, J.P.I., and Nart, F.C., *Langmuir*, 2000, vol. 16, p. 771.
11. Dima, G.E., de Vooys, A.C.A., and Koper, M.T.M., *J. Electroanal. Chem*., 2003, vol. 554-555, p. 15.
12. Pletcher, D., and Poorabedi, Z., *Electrochim. Acta*, 1979, vol. 24, p. 1253.
13. Dima, G.E., Rosca, V., and Koper, M.T.M., *J. Electroanal. Chem*., 2007, vol. 599, p. 167.
14. Shimazu, K., Kawaguchi, T., and Tada, K., *J. Electroanal. Chem*., 2002, vol. 529, p. 20.
15. Tada, K., and Shimazu, K., *J. Electroanal. Chem*., 2005, vol. 577, p. 303.
16. Kerkeni, S., Lamy-Pitara, E., and Barbier, J., *Catalysis Today*, 2002, vol. 75, p. 35.
17. El Omar, F., and Durand, R., *J. Electroanal. Chem*., 1984, vol. 178, p. 343.
18. Markovic, N., Hanson, M., McDougall, G., and Yeager, E., *J. Electroanal. Chem*., 1986, vol.. 214, p. 555.
19. Dima, G.E., Beltramo, G.L., and Koper, M.T.M., *Electrochim. Acta*, 2005, vol. 50, p. 4318.
20. Taguchi, S., and Feliu, J.M., *Electrochim. Acta*, 2007, vol. 52, p. 6023.
21. Taguchi, S., and Feliu, J.M., *Electrochim. Acta*, 2008, vol. 53, p. 3626.
22. Molodkina, E.B., Ehrenburg, M.R., Polukarov, Yu.M., Danilov, A.I., Souza-Garcia, J., and Feliu, J.M., *Electrochim. Acta*, 2010, vol. 56, p. 154.
23. Gomez, R., Yee, H.S., Bommarito, G.M., Feliu, J.M., and Abruna, H.D., *Surf. Sci.*, 1995, vol. 335, p. 101.
24. Molodkina, E.B., Botryakova, I.G., Danilov, A.I., Souza-Garcia, J., and Feliu, J.M., *Rus. J. Electrochem*., 2012, vol. 48, p. 302.
25. Molodkina, E.B., Botryakova, I.G., Danilov, A.I., Souza-Garcia, J., and Feliu, J.M., *Rus. J. Electrochem*., 2013, vol. 49, p. 285.
26. Vidal-Iglesias, F.J., Solla-Gullon, J., Rodríguez, P., Herrero, E, Montiel, V., Feliu, J.M., and Aldaz, A., *Electrochem. Commun*., 2004, vol. 6, p. 1080.
27. Vidal-Iglesias, F.J., Lopez-Cudero, A., Solla-Gullon, J., Aldaz, A., and Feliu, J.M., *Electrocatal.*, 2012, vol. 3, p. 313.
28. Solla-Gullon, J., Vidal-Iglesias, F.J., and Feliu, J.M., *Annu. Rep. Prog. Chem., Sect. C*, 2011, vol. 107, p. 263.
29. Rudnev, A.V., Molodkina, E.B., Ehrenburg, M.R., Fedorov, R.G., Danilov, A.I., Polukarov, Yu.M. and Feliu, J.M., *Rus. J. Electrochem*., 2009, vol. 45, p. 1052.
30. Gisbert, R., Climent, V., Herrero, E., and Feliu, J.M., *J. Electrochem*., 2012, vol. 18, p. 410.
31. Francke, R., Climent, V., Baltruschat, H., and Feliu, J.M., *J. Electroanal. Chem*., 2008, vol. 624, p. 228.
32. Danilov, A.I., Molodkina, E.B., Rudnev, A.V., Polukarov, Yu. M., and Feliu, J.M., *Electrochim. Acta*, 2005, vol. 50, p. 5032.

33. Danilov, A.I., Molodkina, E.B., Rudnev, A.V., Polukarov, Yu.M., Nazmutdinov, R.R., Zinkicheva, T.T., and Feliu, J.M., *Rus. J. Electrochem*., 2008, vol. 44, p. 697.
34. Clavilier, J., *Interfacial Electrochemistry. Theory, Experimental, and Applications*. Ed. A. Wieckowski, N.Y.: Marcel Dekker, Inc., 1999, p. 231.
35. Clavilier, J., Faure, R., Guinet, G., and Durand, R., *J. Electroanal. Chem*., 1980, vol. 107, p. 205.
36. Clavilier, J., *J. Electroanal. Chem*., 1980, vol. 107, p. 211.
37. Domke, K., Herrero, E., Rodes, A., and Feliu, J.M., *J. Electroanal. Chem*., 2003, vol. 552, p. 115.
38. Kibler, L.A., Cuesta, A., Kleinert, M., and Kolb, D.M., *J. Electroanal. Chem*., 2000, vol. 484, p. 73.
39. Danilov, A.I., Molodkina, E.B., Polukarov, Yu. M., Climent, V., and Feliu, J.M., *Electrochim. Acta*, 2001, vol. 46, p. 3137.
40. Vidal-Iglesias, F.J., Solla-Gullon, J., Campina, J.M., Herrero, E., Aldaz, A., and Feliu, J.M., *Electrochim. Acta*, 2009, vol. 54, p. 4459.